Two-Dimensional Subrecoil Laser Cooling

J. Lawall, F. Bardou, B. Saubamea, K. Shimizu,* M. Leduc, A. Aspect,[†] and C. Cohen-Tannoudji

Collège de France et Laboratoire Kastler-Brossel de l'Ecole Normale Supérieure, 24 rue Lhomond,
F-75231 Paris Cedex 05, France
(Received 12 April 1994)

We report the first observation of subrecoil laser cooling in two dimensions by velocity selective coherent population trapping. We have compressed the momentum distribution of a cloud of trapped metastable helium atoms along two orthogonal axes to $\delta p = \hbar k/4$, where $\hbar k$ is the photon momentum. The corresponding temperature, 16 times below the single-photon recoil temperature, is 250 nK. Atoms are pumped into a nonabsorbing state exhibiting four well-resolved momentum peaks with subrecoil widths. The momentum space density in the peaks is significantly greater than that in the uncooled distribution.

One of the goals of laser cooling of atoms is to reach the lowest temperatures possible and accordingly to achieve the largest possible de Broglie wavelengths λ_{dB}. In usual laser cooling schemes [1], fluorescence cycles never cease, so that there are always random recoils due to spontaneously emitted photons. It is then impossible to reach a temperature below the single photon recoil temperature T_R, defined by $k_B T_R/2 = \hbar^2 k^2/2M$, corresponding to the recoil kinetic energy of an atom with mass M absorbing or emitting a single photon with momentum $\hbar k$. There is, however, no fundamental principle preventing laser cooling atoms to below T_R, i.e., with a momentum spread δp smaller than $\hbar k$. This is equivalent to delocalizing the atoms over a de Broglie wavelength λ_{dB} (or more precisely over a spatial coherence length $h/\delta p$) larger than the light wavelength $\lambda_L = 2\pi/k$.

Until now, only two laser cooling schemes [2,3] have allowed subrecoil temperatures to be reached in one dimension [4]. The method of [3] uses sequences of stimulated Raman and optical pumping pulses with appropriate shapes. The approach that forms the basis of the work described here, velocity selective coherent population trapping (VSCPT) [2,5], is based on the combination of two effects: (i) the existence of certain atomic states $|\Psi_p^{NC}\rangle$ which are not coupled to the lasers and which, for p sufficiently small, are perfect traps in momentum space where atoms can remain for very long times, and (ii) a random walk of the atoms in momentum space, due to exchanges of momentum with photons during fluorescence cycles, which allows atoms to diffuse from nontrapping states with $p \neq 0$ to trapping states with $p \cong 0$ where they accumulate. According to the theoretical analysis [5], the momentum width δp of the cooled atoms should decrease without fundamental limit as $1/\sqrt{\Theta}$, where Θ is the laser-atom interaction time. Recently, a new generation VSCPT experiment [6], using precooled He* atoms released from a trap, has allowed us to achieve 1D cooling to $\delta p \simeq \hbar k/4.5$, i.e., an equivalent temperature [7] $T_R/20$ (200 nK in the case of He*).

The generalization of subrecoil cooling to two and three dimensions is a crucial issue [8]. Several 2D generalizations of VSCPT have been proposed [5,9,10]. In this paper, we present the first experimental realization of two-dimensional VSCPT cooling, carried out with the new He* apparatus of Ref. [6]. We have obtained cooled atoms with a momentum distribution half-width $\delta p \simeq \hbar k/4$ along any direction in the cooling plane. The corresponding effective temperature [6] is $T_R/16$.

We now briefly explain how VSCPT can be extended to two or three dimensions for $J_g = 1 \longrightarrow J_e = 1$ transitions, following the presentation of Ref. [10]. In the lower state g, the atom can be considered as a spin one particle, because $J_g = 1$. Consequently, its state is described by a wave function $\Psi(\mathbf{r})$, which is a vector field. Similarly, the state of the atom in the excited state e (with $J_e = 1$) is described by a vector field $\Phi(\mathbf{r})$. Finally, there is in the atom-laser interaction Hamiltonian V_{AL} a third vector field, the laser electric field $\mathbf{E}_L(\mathbf{r})$. The transition amplitude induced by V_{AL} between g and e may be shown to be proportional to the following integral:

$$\int d^3 r \, \Phi^*(\mathbf{r}) \cdot [\mathbf{E}_L(\mathbf{r}) \times \Psi(\mathbf{r})], \tag{1}$$

which is in fact the only scalar which can be constructed from the three vector fields $\Phi^*(\mathbf{r})$, $\mathbf{E}_L(\mathbf{r})$, and $\Psi(\mathbf{r})$. As in the one-dimensional case, a perfect trapping state in g, $\Psi^T(\mathbf{r})$, is defined by two conditions [5]. First, it must not be coupled by V_{AL} to the excited state. The integral (1), with $\Psi(\mathbf{r})$ replaced by $\Psi^T(\mathbf{r})$, must be equal to zero for all $\Phi(\mathbf{r})$. Second, $\Psi^T(\mathbf{r})$ must be an eigenfunction of the kinetic energy Hamiltonian $\mathbf{P}^2/2M$. Such a condition ensures that the state $\Psi^T(\mathbf{r})$ will not be destabilized by a motional coupling induced by $\mathbf{P}^2/2M$ between $\Psi^T(\mathbf{r})$ and other ground states coupled to e. It is then easy to see that the state

$$\Psi^T(\mathbf{r}) = \alpha \mathbf{E}_L(\mathbf{r}), \tag{2}$$

where α is a c-number, fulfills these two conditions. First, the two vector fields $\Psi^T(\mathbf{r})$ and $\mathbf{E}_L(\mathbf{r})$ being parallel, we

have $E_L(\mathbf{r}) \times \Psi^T(\mathbf{r}) = 0$ for all $\mathbf{r}$. Second, since $E_L(\mathbf{r})$ is a monochromatic laser field with frequency ω_L, all wave vectors $\mathbf{k}_i$ appearing in the plane wave expansion of $E_L(\mathbf{r})$,

$$E_L(\mathbf{r}) = \sum_{i=1}^{N} \mathcal{E}_{oi} \hat{\boldsymbol{\epsilon}}_i \exp(i\mathbf{k}_i \cdot \mathbf{r}), \qquad (3)$$

have the same modulus $|\mathbf{k}_i| = \omega_L/c = k$. Using the same expansion for $\Psi^T(\mathbf{r})$ given in (2), we find that the atomic kinetic energy $\mathbf{P}^2/2M$, which depends only on the modulus of the wave vectors, has a well-defined value in $\Psi^T(\mathbf{r})$ equal to $\hbar^2 k^2/2M$. If we replace in (2) the c-number α by an arbitrary scalar field $\alpha(\mathbf{r})$, we still have $E_L(\mathbf{r}) \times \Psi^T(\mathbf{r}) = 0$ for all $\mathbf{r}$, so that $\alpha(\mathbf{r})E_L(\mathbf{r})$ is the most general state in g not coupled to e, i.e., leading to a zero transition amplitude (1) for all $\Phi(\mathbf{r})$. Expanding $\alpha(\mathbf{r})$ in plane waves $\exp(i\mathbf{p} \cdot \mathbf{r}/\hbar)$, we introduce a set of noncoupled states,

$$\Psi_{\mathbf{p}}^{NC}(\mathbf{r}) = E_L(\mathbf{r}) \exp(i\mathbf{p} \cdot \mathbf{r}/\hbar) \qquad (4)$$

labeled by $\mathbf{p}$. Equations (3) and (4) then show that $\Psi_{\mathbf{p}}^{NC}(\mathbf{r})$ is a linear superposition of plane waves with wave vectors $\mathbf{k}_i + \mathbf{p}/\hbar$. In general, these wave vectors do not have the same modulus, and (4) is not an eigenfunction of $\mathbf{P}^2/2M$. There are motional couplings, proportional to $\mathbf{k}_i \cdot \mathbf{p}/M$, which destabilize the states (4) and introduce a photon absorption rate $\Gamma'_{NC}(\mathbf{p})$ from these states proportional to $\mathbf{p}^2$ (if $|\mathbf{p}|$ is small enough) [5,11]. Such an absorption is then followed by a spontaneous emission process, which introduces a random change of momentum and allows atoms to diffuse in momentum space. The smaller $|\mathbf{p}|$, the smaller is the diffusion rate. Atoms thus progressively accumulate in a set of states $\Psi_{\mathbf{p}}^{NC}(\mathbf{r})$, with $|\mathbf{p}|$ distributed over a range δp around the value $\mathbf{p} = 0$ corresponding to the perfectly dark state (2). Arguments similar to those used in [5] show that δp decreases as $1/\sqrt{\Theta}$ where Θ is the interaction time.

We now apply these general considerations to the laser configuration used in our experiment. It consists of counterpropagating beams along the x and y axes, with σ^+ and σ^- polarizations (Fig. 1). In Eq. (3) we have $N = 4$ and $\mathbf{k}_1 = k\hat{x}$, $\mathbf{k}_2 = -k\hat{x}$, $\mathbf{k}_3 = k\hat{y}$, and $\mathbf{k}_4 = -k\hat{y}$. It is then clear that for any $\mathbf{p}$ orthogonal to the x-y plane the four vectors $\mathbf{k}_i + \mathbf{p}/\hbar$ have the same modulus, so that there is no velocity selection and thus no cooling along the z axis. On the other hand, the reasoning above shows that there is velocity selection for $\mathbf{p}$ in the x-y plane, where the only trapping state of the form (4) is $\Psi_{\mathbf{p}}^{NC}$ with $\mathbf{p} = 0$. Furthermore, one can show [10] that with the polarization configuration of Fig. 1 there is a unique two-dimensional trapping state. We thus expect that, after the laser configuration of Fig. 1 has been applied for a time Θ to an atom, the state of the atom will be of the form (4) with a $\mathbf{p}$ component in the x-y plane very close to 0 ($|\mathbf{p}|$ less than $\hbar k$) and an arbitrary value for p_z. This state will thus consist of four coherent wave packets with mean momenta $\pm\hbar k\hat{x}$, $\pm\hbar k\hat{y}$. Thus, on the detection plane,
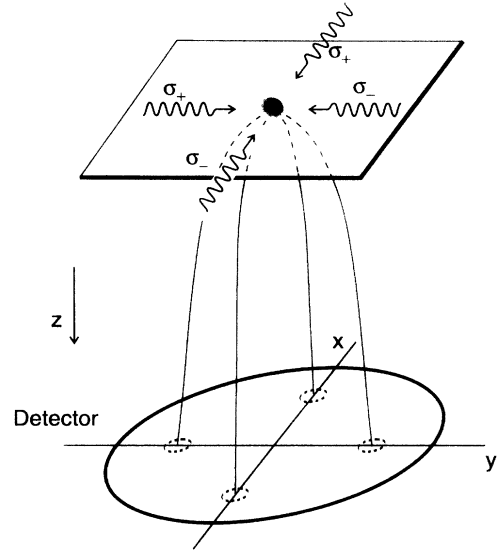
FIG. 1. 2D VSCPT scheme. Under the influence of the four VSCPT cooling beams, the atoms are pumped into a coherent superposition of four wave packets whose centers follow ballistic trajectories to the position-sensitive detector 5 cm below.

one should observe four spots separated by a distance $2\hbar k\tau_f/M$, where τ_f is the time of flight to the detector, the width of these spots decreasing as $1/\sqrt{\Theta}$.

In order to have real cooling, one needs to fill the trapping state with sufficient efficiency. As shown in [11], a pure diffusion in momentum space is much less efficient in two dimensions than in one dimension. On the other hand, as emphasized in [9], 2D VSCPT schemes on a $J_g = 1 \longleftrightarrow J_e = 1$ transition may lead to a friction force for atoms which are not yet trapped. There is then a drift toward $\mathbf{p} = 0$ which helps to fill the trapping states [12]. Although we have not yet made any detailed calculations, we expect, based on the fact that the light shifts in our laser configuration are spatially dependent, that VSCPT efficiency would be augmented by Sisyphus precooling for the case of blue detuning [1].

We start with atoms precooled to $\sim200\,\mu$K in a magneto-optical trap [13,14]. A cryogenic (6 K) beam of He* in the $2\,^3S_1$ state is decelerated by radiation pressure using a Zeeman slowing technique [15] to load the trap. Our trap contains $\sim10^5$ atoms in a volume of ~1 mm^3. The trap is shut off, and the beams for the VSCPT cooling process, tuned to the $2\,^3S_1 - 2\,^3P_1$ transition, are pulsed on (Fig. 1). All of the VSCPT laser beams are derived from the same laser, so the phase coherence is limited by the stability of the retroreflection mirrors. During the time of the VSCPT cooling, the atoms move less than 1 mm, after which they follow ballistic trajectories under the influence of gravity. Atoms are detected 5 cm below the trap by means of a microchannel plate detector which intercepts a solid angle of 0.32 sr. High spatial resolution (0.5 mm) is obtained by accelerating the output of the microchannel plates toward a phosphor screen, and

the resulting blips of light are recorded with a triggered charge coupled device (CCD) camera which provides temporal resolution.

The detailed sequence is the following: The trap is loaded for about 1.5 s, at which point the deceleration coils are turned off while the quadrupole trapping coils remain on. This allows the magnetic fields of the deceleration coils to decay, during which time the trap laser parameters are adjusted to provide further cooling. After 250 ms, the trapping coils are switched off as well, and the trapping laser beams are left on for an additional 3.5 ms. This phase confines the atoms in an optical molasses while allowing the residual fields of the quadrupole to decay. At this point, the trapping beams are turned off and the VSCPT cooling beams are switched on. The VSCPT interaction time is 500 μs in the work described here. Atoms are detected on the microchannel plate detector a time τ_f (30–70 ms) later within a temporal window τ which can be as small as 1 ms. By varying τ_f we can probe the (uncooled) vertical velocity distribution, and by varying τ we can select the time resolution. Images from the CCD camera are digitized in a PC, and successive images are summed.

Simple arguments [6] show that the temperature attainable is limited by the stray magnetic field and scales as the square of the field; a stray field on the order of 1 mG limits the achievable temperature to $\sim T_R/100$. The ac components of the magnetic field at 50 Hz ($\sim$10 mG) are reduced to less than 1 mG by means of a Mumetal shield. The static components are canceled *in situ* and at the time
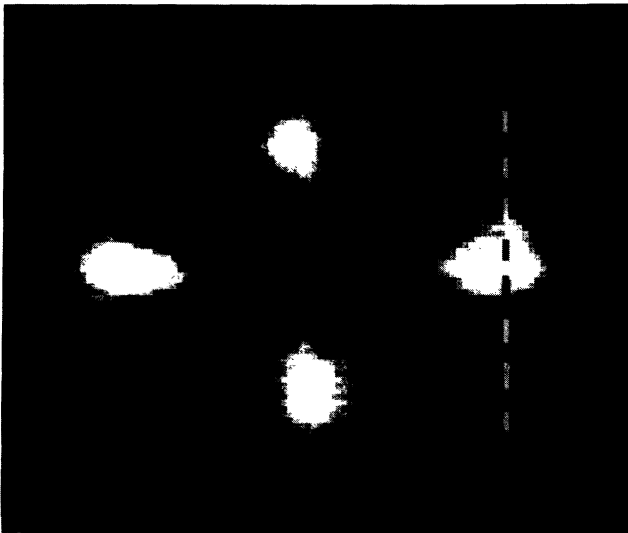
of interest to within 0.5 mG by means of an additional step based on the mechanical Hanle effect [16].

An image of the atomic position distribution detected on the microchannel plate is shown in Fig. 2. The four peaks are clearly resolved. The widths of the peaks reflect, in addition to the final VSCPT momentum distribution, contributions due to the size of the cloud of trapped atoms, the size of the blips of light emitted by the phosphor, and the dispersion of atom arrival times during the observation time τ. The latter broadening mechanism is absent in the direction perpendicular to the recoil momentum. With this in mind, we present in Fig. 3 a vertical profile through the peak at the right in Fig. 2. An upper bound to the momentum dispersion is given by neglecting the initial cloud size and the imperfect detector resolution [17]. From the width of the peak, we deduce a velocity spread (half-width at $1/\sqrt{e}$) of 2.3 cm/s ($= v_R/4$, where $v_R = \hbar k/M = 9.2$ cm/s is the recoil velocity), with an uncertainty of 10%. The corresponding temperature is $T_R/16$.

A crucial issue is whether the VSCPT process actually increases the density in momentum space or merely acts to *select* atoms within a small velocity group. The answer is dependent on the laser parameters. For a fixed value of the detuning $\delta \simeq +0.5\Gamma$, a scan of the laser power (Rabi frequency Ω varying from $\Omega \simeq 0.5\Gamma$ to $\Omega \simeq 1.06\Gamma$) revealed both a monotonically increasing temperature and a number of cooled atoms. The smallest laser power, while giving the narrowest velocity distribution ($T \simeq T_R/30$), yielded fewer atoms in the peak than in the absence of the VSCPT cooling process. We interpret this expulsion of atoms as being due to heating from a "blue Doppler molasses" [1] before atoms are trapped in the velocity-selective state. As the laser power is increased, the distributions are observed to broaden

FIG. 2. Image of the detected atomic position distribution for the experimental parameters: Rabi frequency $\Omega \simeq 0.8\Gamma$, detuning $\delta \simeq +0.5\Gamma$, interaction time $\Theta = 500$ μs. The figure shows an integration of 25 consecutive images for each of which the camera was exposed from 45 to 65 ms after the VSCPT interaction. The corresponding momentum distribution consists of four peaks at $\pm\hbar k$ along the x and y axes; the peak widths are clearly subrecoil.

FIG. 3. Profiles of the atomic position distributions along the dotted line of Fig. 2 with and without VSCPT cooling.

somewhat but to contain many more atoms. The increase in the temperature as the Rabi frequency is raised is qualitatively in accord with theoretical predictions [5]. At a threshold of about $\Omega \simeq 0.7\Gamma$ the density of atoms in the peak is rougly equal to that observed without VSCPT cooling. The data shown in Fig. 3 were taken at $\Omega \simeq 0.8\Gamma$. The dotted line shows the profile taken in the absence of VSCPT cooling. The peak is 3 times higher than the uncooled atomic distribution; moreover, atoms are clearly removed from nearby velocity states. Keeping the Rabi frequency at $\Omega = 0.8\Gamma$ and increasing the detuning provides still greater accumulation; at a detuning of about $\delta \simeq +1.8\Gamma$ the peak rises a factor of 10 over the signal in the absence of VSCPT, although the temperature is somewhat higher at $T \simeq T_R/12$. The enhanced accumulation of atoms at higher laser powers is understood as being due to an increase in the fluorescence rate [11], while the enhancement at greater detuning is expected to be a consequence of additional Sisyphus-type friction mechanisms [9,12].

We have demonstrated here that VSCPT is a practical means of achieving subrecoil laser cooling in two dimensions, providing significant enhancement of the density in momentum space. The final temperature we have observed corresponds to a de Broglie wavelength of $4 \mu m$. When the factors (stray magnetic fields, phase stability of the standing waves, polarization quality, laser power, detuning) determining the final temperature and fraction of cooled atoms are under control, we expect that by increasing the VSCPT interaction time to several milliseconds we should be able to reduce the temperature by another order of magnitude. We note as well that atoms are prepared in a coherent superposition of wave packets whose centers, in our work, are separated by a macroscopic distance on the order of 1 cm. An obvious challenge is to recombine the four beams of Fig. 2 in order to observe interference and thus demonstrate the coherence. In the near future we plan to use the same approach to accomplish three-dimensional subrecoil cooling.

---

*Present address: Department of Applied Physics and Chemistry, The University of Electro-Communications, 1-5-1 Chofugaoka, Chofu, Tokyo 182, Japan.
†Present address: Institut d'Optique Théorique et Appliquée, B.P. 147, 91403 Orsay Cedex, France.

[1] For an overview of laser cooling see, e.g., C. Cohen-Tannoudji, in Fundamental Systems in Quantum Optics, Proceedings of the Les Houches Summer School, Session LIII, edited by J. Dalibard, J.-M. Raimond, and J. Zinn-Justin (North-Holland, Amsterdam, 1992), p. 1.

[2] A. Aspect, E. Arimondo, R. Kaiser, N. Vansteenkiste, and C. Cohen-Tannoudji, Phys. Rev. Lett. 61, 826 (1988).

[3] M. Kasevich and S. Chu, Phys. Rev. Lett. 69, 1741 (1992).

[4] See also the proposals described by D.E. Pritchard, K. Helmerson, V.S. Bagnato, G.P. Lafyatis, and A.G. Martin, in Laser Spectroscopy VIII, edited by W. Persson and S. Svanberg (Spinger-Verlag, Berlin, 1987); H. Wallis and W. Ertmer, J. Opt. Soc. Am. B 6, 2211 (1989); K. Mølmer, Phys. Rev. Lett. 66, 2301 (1991).

[5] A. Aspect, E. Arimondo, R. Kaiser, N. Vansteenkiste, and C. Cohen-Tannoudji, J. Opt. Soc. Am. B 6, 2112 (1989).

[6] F. Bardou, B. Saubamea, J. Lawall, K. Shimizu, O. Emile, C. Westbrook, A. Aspect, and C. Cohen-Tannoudji, C. R. Acad. Sci. Ser. 2 318, 877 (1994).

[7] Strictly speaking, it is not possible to assign a temperature in the present case; the momentum distribution is not Gaussian and exhibits several peaks and does not tend toward a steady state. Nevertheless, we can define a temperature as a convenient indicator of the width δp individual momentum groups via the expression $kT/2 = \delta p^2/2M$. Here, in analogy with the usual thermodynamic situation, we take δp to be the half-width at $1/\sqrt{e}$ of the momentum distribution along any chosen direction.

[8] The Raman cooling scheme of Ref. 3 has been generalized to two and three dimensions: N. Davidson, H.-J. Lee, M. Kasevich, and S. Chu, Phys. Rev. Lett. 72, 3158 (1994). Although they do not claim subrecoil cooling, the use of the definition of Ref. 7, applied to their results, yields a temperature slightly below T_R in two dimensions.

[9] F. Mauri and E. Arimondo, in Proceedings of Light Induced Kinetic Effects, edited by L. Moi et al. (ETS Editrice, Pisa, 1991); F. Mauri and E. Arimondo, Europhys. Lett. 16, 717 (1991).

[10] M.A. Ol'shanii and V.G. Minogin, in Proceedings of Light Induced Kinetic Effects, edited by L. Moi et al. (ETS Editrice, Pisa, 1991); M.A. Ol'shanii and V.G. Minogin, Opt. Commun. 89, 393 (1992).

[11] F. Bardou, J.P. Bouchaud, O. Emile, A. Aspect, and C. Cohen-Tannoudji, Phys. Rev. Lett. 72, 203 (1994).

[12] The interest of a friction force has also been stressed by E. Korsunsky et al., Phys. Rev. A 48, 1419 (1993); M.S. Shahriar et al., ibid., R4035 (1993); P. Marte et al., ibid., Phys. Rev. A 49, 4826 (1994).

[13] E.L. Raab, M. Prentiss, A. Cable, S. Chu, and D.E. Pritchard, Phys. Rev. Lett. 59, 2631 (1987).

[14] F. Bardou, O. Emile, J.-M. Courty, C.I. Westbrook, and A. Aspect, Europhys. Lett. 20, 681 (1992).

[15] W.D. Phillips and H. Metcalf, Phys. Rev. Lett. 48, 596 (1982).

[16] R. Kaiser, N. Vansteenkiste, A. Aspect, E. Arimondo, and C. Cohen-Tannoudji, Z. Phys. D 18, 17 (1991).

[17] The radii of the cloud of trapped atoms and the sizes of the blips of light are each about 0.5 mm, and so contribute about 25% of the width of the detected peak. Thus the actual temperature may reasonably be expected to be of the order of 30% lower than the raw result quoted in the text.
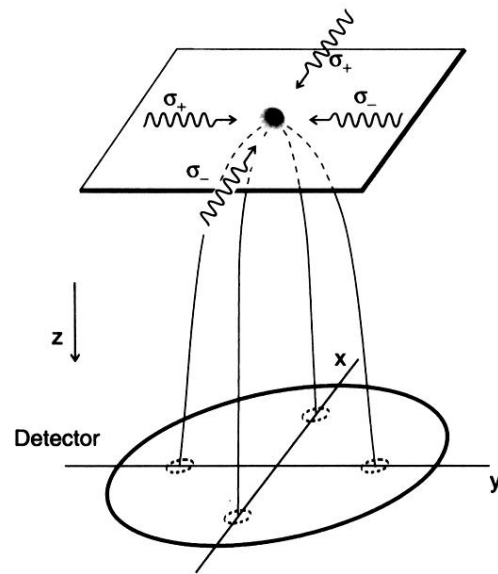
FIG. 1. 2D VSCPT scheme. Under the influence of the four VSCPT cooling beams, the atoms are pumped into a coherent superposition of four wave packets whose centers follow ballistic trajectories to the position-sensitive detector 5 cm below.
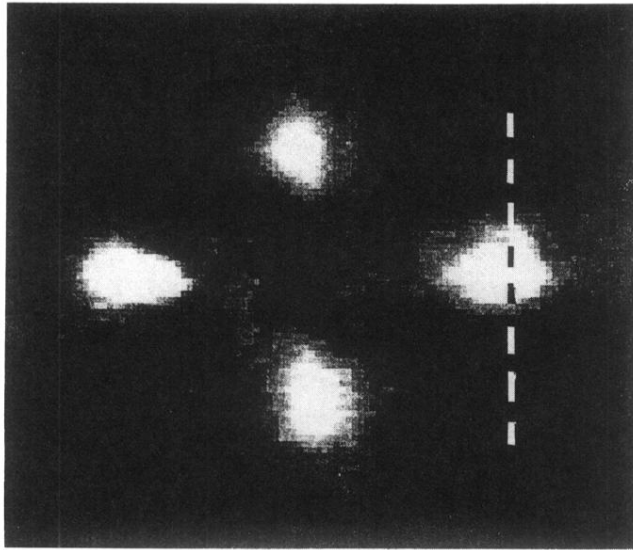
FIG. 2. Image of the detected atomic position distribution for the experimental parameters: Rabi frequency $\Omega \simeq 0.8\Gamma$, detuning $\delta \simeq +0.5\Gamma$, interaction time $\Theta = 500 \ \mu$s. The figure shows an integration of 25 consecutive images for each of which the camera was exposed from 45 to 65 ms after the VSCPT interaction. The corresponding momentum distribution consists of four peaks at $\pm\hbar k$ along the x and y axes; the peak widths are clearly subrecoil.